Multi-debris Removal in Low-Orbit Based on Swarm Intelligence Research on Optimal Guidance Method

Na Fu(✉), Tian-Jiao Zhang, Lai-Jian Zhou, Yan-Yan Zeng, and Chen Zhang

State Key Laboratory of Astronautic Dynamics, Xi'an Satellite Control Center, Xi'an 710049, Shaanxi, China
40365728@qq.com

Abstract. Low-orbit space debris removal path planning can be decomposed into optimization problems of debris removal sequences and optimization of transfer orbit design between debris. In this paper, a two-level planning model is established, and the corresponding group intelligent optimization algorithm is proposed. The upper-level optimization problem takes the debris removal sequence as the design variable, considers the task time constraints, and takes the minimum total task energy consumption as the optimization goal, and uses the discrete ant colony algorithm to solve the optimal debris removal sequence. The lower optimization problem takes the maneuvering time and impulse of the inter-debris transfer orbit mission as the design variables, considers the influence of the earth's non-spherical perturbation, and adopts the single-circle perturbation Lambert algorithm for the constraint processing method of terminal state satisfaction, and proposes a method based on continuous ant colony. Optimized path planning algorithm. Simulation results show that the strategy and algorithm proposed in this paper are efficient and feasible, which can save fuel to the greatest extent and maximize the benefits of space debris mitigation. The research results of this paper provide technical reserves for the follow-up exploration of the integrated design optimization of debris transfer orbits and debris removal sequences.

Keywords: Debris removal · Path planning · Swarm intelligence · Global optimization

1 Introduction

The continuous growth of space debris makes the space environment worse and worse, affecting the normal space activities of human beings. Especially for the near-Earth region [1–10], nearly 90% of the cataloged space targets are debris, and its distribution is relatively dense, which is prone to debris cascading collision effects. Figure 1 shows a schematic diagram of space debris. NASA scientist Kessler [9] pointed out that even if the mission spacecraft is no longer launched, the number of debris will continue to increase due to the mutual collision between the debris. This will seriously threaten the safe operation of spacecraft such as orbiting satellites and space stations. Therefore, low-cost and high-efficiency active debris removal is urgent and necessary [4–7].

Q. Wu et al. (Eds.): WiSATS 2020, LNICST 358, pp. 116–131, 2021.
https://doi.org/10.1007/978-3-030-69072-4_10

Fig. 1. Schematic diagram of space debris in Earth orbit

Since the orbital distribution of the most threatening debris may be scattered, making the cost of active debris removal missions high, consideration should be given to both the cost of removal and the benefits of removal. Decisions such as debris removal, optimization of debris removal timing, and optimal maneuvering strategy for spacecraft removal should be preferred. The collaborative optimization makes the low-orbit multi-debris removal path planning problem exhibit the characteristics of mixed integer nonlinear planning, and the continuous movement of space debris makes the energy consumption for the transfer of debris time-varying, which increases the difficulty of solving the problem.

In 1986, China included space debris research as one of the important space environmental factors facing manned spaceflight, and included it in the environmental protection plan. In 1995, China officially joined the IADC to carry out systematic research on space debris. Regarding the research on the space debris environment model, in the "Space Debris Environment Detector and Engineering Model Research" project during the 12th Five-Year Plan period, Harbin Institute of Technology undertook the establishment of a space debris environment debris environment model [3]. At present, the project has completed the investigation of modeling principles of typical space debris environment models at home and abroad, and compared and analyzed the typical space debris models published abroad. China carries out detailed analysis and research on foreign space debris generation event models, and establish a space debris orbit evolution model. The modeling method of the environmental engineering model of space debris in low-Earth orbit has been preliminarily established. China is still in the exploratory stage in predicting the future evolution of space debris environment and has not yet released a mature model or algorithm. Existing modeling methods and theoretical research also need to be improved, and there is a big gap with foreign countries. The establishment of China's autonomous space debris environmental engineering model requires the prediction of space debris environmental evolution.

At present, there are only a few articles on the optimal design strategy of multi-shard intersection. Barbee et al. [11] ignored the impact of J2 perturbation, considered a simplified two-body orbit transfer model, and described the removal path planning problem

given a set of low-orbit debris to be removed as a static traveling salesman (Traveling Salesman Problem, TSP) problem, using order The optimization algorithm solves and compares the debris removal efficiency of different spacecraft loads and engine ratios. Cerf et al. [12] studied the clearance path planning of five low-orbit debris under the condition of considering J2 perturbation. By giving alternative drift orbit parameters to remove time-related factors, the branch and bound method was used to obtain the optimal Debris removal timing and corresponding orbit transfer path. Olympio et al. [13] studied the problem of the most energy-efficient removal of the five fragments of the solar synchronous orbit, discretized the possible start time interval of the task, the feasible time interval of the orbit transfer, and the allowable time interval of the orbit drift, determined the parameter combination for each group, and adopted The small thrust J2 perturbed the Lambert algorithm [15] to obtain the energy consumption of small thrust orbit transfer between any debris, and finally use the branch and bound algorithm to search for the optimal removal timing and removal path. From the publicly reported literature, the existing research usually performs two-body simplification and gives the debris removal time and calculates the corresponding transfer energy consumption, or discretizes the possible debris removal time and then conducts a grid search, and then models it as TSP Or solve its deformation model. However, due to the long period of debris removal tasks, usually in years, for the LEO debris removal task, the impact of J2 perturbation on the debris orbit cannot be ignored, and the two-body simplification is obviously unreasonable. However, the research based on grid search does not accurately estimate the optimal debris removal time and the corresponding energy consumption of orbital transfer, and its computational cost increases exponentially with the increase in the number of candidate debris. Supercomputer-assisted or manual correction is required to achieve the calculation It is difficult to generalize, so it cannot be used to solve the sequential removal path planning of large-scale candidate debris. In this paper, with the background of low-orbit multi-debris removal path design optimization as the background, a two-layer optimization framework is proposed: the upper layer optimization takes the order of debris removal as the design variable, considers the task time constraint, and takes the minimum total task energy consumption as the optimization goal, using the discrete ant colony algorithm Solve the optimal debris removal sequence; the lower-level optimization problem takes the maneuvering time and impulse of the inter-debris transfer orbit task as the design variables, considers the influence of J2 perturbation, and adopts the single-circle perturbation Lambert algorithm for the constraint processing method of terminal state satisfaction. A path planning algorithm based on continuous ant colony optimization.

2 Low Orbit Space Debris Removal Mission Scenes

2.1 Distribution and Evolution of Space Debris in Low Earth Orbit

There have been nearly 6,000 spacecraft launched into orbit in human history, most of which are distributed in low-Earth orbits below 2000 km in altitude and geosynchronous orbits at an altitude of about 36,000 km. Some man-made objects have returned to the atmosphere Falling and destroying, but most of them still remain in the earth's orbit. From the spatial distribution, most of them are distributed in the LEO area. And in the

LEO area, it is most distributed in an area of 8,000 km. Figure 2 shows the distribution of the number of space debris with the semi-major axis and the orbital inclination angle in December 2016. In the figure, the interval of orbital inclination is 2°, and the interval of semi-major axis is 100 km. It can also be seen intuitively from Fig. 2 that space debris is mainly concentrated in low-Earth orbits, synchronous orbits, and some mid-high orbit regions.

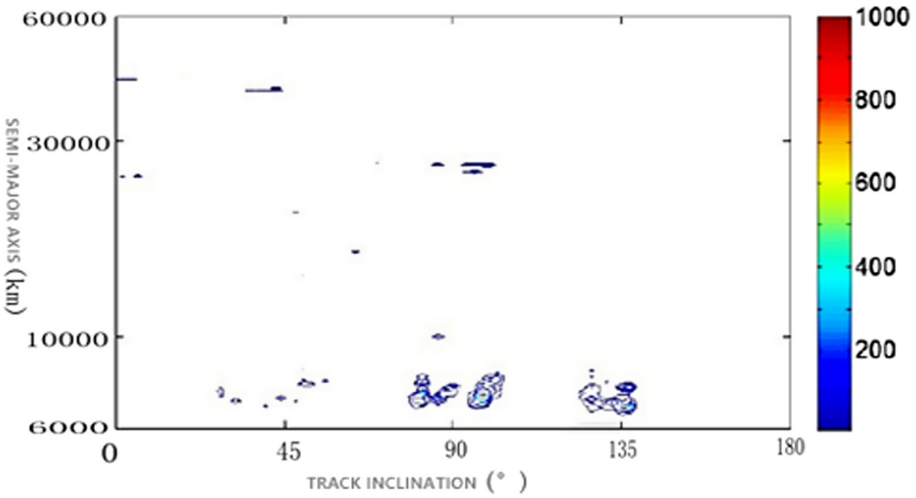

Fig. 2. Space debris distribution

2.2 Low-Orbit Space Debris Removal Mission Scenario

Currently, the generally accepted scenario for active debris removal is shown in Fig. 3. At the initial moment, a spacecraft carrying several debris removal devices is launched to a designated orbital position, usually coincident with the first preferred debris position. The clearing spacecraft meets with the first preferred debris. With the flight and release of the clearing device, the de-orbital removal of the debris is the responsibility of the clearing device, and then the clearing of the spacecraft departs, and the successive debris removal and removal of the preferred debris until the spacecraft propellant consumption is cleared After all or all of the preferred debris removal is completed, the sequential debris removal task ends.

Because the orbital distribution of the preferred debris may be scattered, if the clear spacecraft directly carries out pulse orbit transfer between the debris, it usually needs to consume more speed increments. Therefore, in order to ensure the successful completion of the sequential debris removal task, for the sequential debris removal task without orbit transfer time constraints, the influence of J2 natural perturbation on the right ascension of the ascending intersection point should be fully adjusted to adjust the orbital surface deviation, so as to effectively reduce the orbit transfer The purpose of energy consumption. In this paper, the debris removal task that uses only J2 natural perturbation to adjust

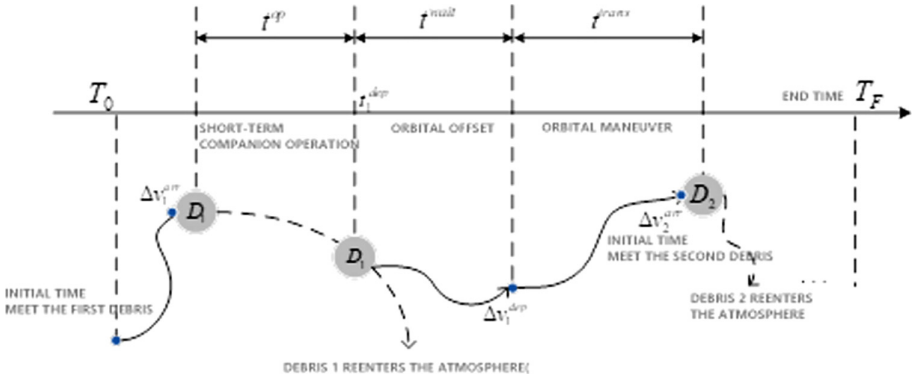

Fig. 3. Debris removal mission scenario

the difference in right ascension between the spacecraft and the debris ascending point is called the debris removal task of natural perturbation of the right ascension. Specifically, for the sequential debris removal task of the natural perturbation of the right ascension, after the spacecraft has cleared a certain preferred debris, it needs to perform an orbit drift for a period of time, through J2 natural perturbation to make the intersection point of right ascension and subsequent preferred debris The right ascension coincides. At this time, the orbit maneuver only needs to adjust the inclination of the orbit and the in-plane orbit change, so the most energy-saving.

3 Path Planning Model for Low-Orbit Space Debris Removal

The low-orbit space debris removal path planning problem has characteristics such as multi-minimum values, search space discontinuity, and multi-scale. Therefore, this section adopts the solution strategy of hierarchical modeling serial planning. The upper layer plan is used to determine the optimal removal order, and the lower layer plan is used to determine the optimal multi-pulse transfer path between two adjacent target fragments.

3.1 Upper Level Optimization Model

The goal of the upper-level planning problem is to determine the optimal removal order of the target debris, so that the total energy consumption of the orbital transfer of the debris removal by the spacecraft in order is minimized. Since the energy consumption of the spacecraft's orbital transfer between any two target fragments is determined by the lower layer planning, if the precise solution of the lower layer planning is used as the input for the upper layer planning, the solution algorithm has a high time complexity. In view of this, this paper designs a method for estimating the orbital energy consumption and time between target debris of a spacecraft that does not rely on lower level planning, to decouple upper and lower level planning, and to quickly determine the optimal removal order.

3.1.1 Energy Consumption and Time Estimation Method for Orbital Transfer Between Target Fragments

The energy consumption of orbital transfer between target debris is composed of the energy consumption of plane-free orbit change and the energy consumption of in-plane orbit change. This section makes full use of the impact of long-term perturbation of J2 on the right ascension of the ascending intersection point. After the spacecraft has cleared a debris, it drifts for a period of time. The natural ascension force causes the right ascension of the ascending intersection point to coincide with the debris of the debris to be met. At this time, the spacecraft and the debris to be removed have similar orbital inclination angles and the same ascension point of right ascension. Therefore, tracking spacecraft only needs to perform different plane orbit changing maneuvers and pulse adjustment camera movements with lower energy consumption to be able to locate with the debris to be removed.

The energy consumption of orbit changing in different planes is mainly used to adjust the inclination of the track, so it can be estimated by the following formula:

$$\Delta v_{inter} \approx 2v \sin(\Delta i/2) \tag{1}$$

Δv_{inter} is the estimated energy consumption for different plane orbit changes; v is the speed of the spacecraft before the orbit change; Δi is the estimated energy consumption for different plane orbit changes.

Among the orbital transfers between two coplanar elliptical orbits, the Homan transfer is the most energy-efficient double-pulse maneuver. Since the spacecraft's transfer time between debris is long enough, it is assumed that it can always be adjusted to the optimal phase to perform the Homan transfer before in-plane orbit transfer, so the in-plane between target debris is estimated by the energy consumption of the Homan transfer The energy consumption of track change is as follows:

$$\Delta v_{intra} \approx 0.5v\sqrt{(\Delta a/a)^2 + \Delta e^2} \tag{2}$$

Δv_{intra} Estimated energy consumption for in-plane orbit change; a, v the semi-major axis and velocity of the spacecraft before orbit change, respectively Δe is the difference in eccentricity between the two orbits.

3.1.2 Debris Removal Order Optimization Model

When the method described in Sect. 3.1.1 is used to estimate the spacecraft orbital transfer energy between two debris, the cleaning sequence optimization problem with the smallest total energy consumption can be abstracted as a classic TSP problem solution. The upper-level removal order optimization problem can be defined as searching for the shortest Hamilton path in the complete graph $G = <V, E>$, where V is the set of debris to be removed, $E = \{e_{ij} \mid d_i, d_j \in V\}$ is the set of edges G in the graph, $|V| = n$; and the length of the edge c_{ij} is set to the estimated energy of the spacecraft's orbital transfer between the two debris Consumption, the shortest Hamilton path in the figure G corresponds to the multi-debris removal sequence with the smallest total energy consumption.

x_{ij} is Boolean decision variable, used to characterize whether the spacecraft continuously removes debris d_i, d_j, if e_{ij} is in the shortest Hamilton Road, $x_{ij} = 1$; otherwise $x_{ij} = 0$.

The problem is modeled using the 0–1 integer programming model as follows:

$$\begin{aligned} \min \quad & \sum_{i=1}^{n}\sum_{j=1}^{n} c_{ij}x_{ij} \\ s.t. \quad & \sum_{i=1}^{n} x_{ij} \le 1, j = 2, \ldots, n \\ & \sum_{j=1}^{n} x_{ij} \le 1, i = 2, \ldots, n \\ & x_{ij} \in \{0, 1\}, \ \forall e_{ij} \in E \end{aligned} \tag{3}$$

3.2 Lower Level Optimization Model

On the basis of determining the optimal clearance order in the upper layer planning, the lower layer planning needs to optimize the precise path of the multi-pulse transfer between two adjacent debris according to the optimal clearance order.

3.2.1 Kinetic Model

Since spacecraft and debris are both in the vicinity of LEO orbit, only the gravitational effect of the earth is considered. The orbital dynamic equation of spacecraft under J2 perturbation described by the number of orbits is:

$$\begin{cases} \frac{\mathrm{d}a}{\mathrm{d}t} = 0 \\ \frac{\mathrm{d}e}{\mathrm{d}t} = 0 \\ \frac{\mathrm{d}i}{\mathrm{d}t} = 0 \\ \frac{\mathrm{d}\Omega}{\mathrm{d}t} = -\frac{3}{2}\frac{nJ_2\cos i}{(1-e^2)^2}\left(\frac{R_e}{a}\right)^2 \\ \frac{\mathrm{d}\omega}{\mathrm{d}t} = -\frac{3nJ_2[1-5\cos^2 i]}{4(1-e^2)^2}\left(\frac{R_e}{a}\right)^2 \\ \frac{\mathrm{d}M}{\mathrm{d}t} = n + \frac{3nJ_2[3\cos^2 i-1]}{4(1-e^2)^{3/2}}\left(\frac{R_e}{a}\right)^2 \end{cases} \tag{4}$$

Number of orbits $E = (a, e, i, \Omega, \omega, M)$ represent the semi-major axis of the spacecraft orbit, eccentricity, orbital inclination, right ascension of the ascending intersection point, the perigee amplitude angle, and the meso point angle; J_2 is the second harmonic; R_e is earth radius.

3.2.2 Model of Spacecraft Transfer Path Planning Between Adjacent Debris

The spacecraft uses drift and four-pulse maneuvers to meet space debris. Taking the q path planning for the intersection with the first debris as an example, the lower-level optimization uses four maneuvers and the impulse as design variables:

$$y_q = \left(\Delta t_{q1}, \Delta t_{q2}, \Delta t_{q3}, \Delta t_{q4}, \Delta \mathbf{v}_{q1}, \Delta \mathbf{v}_{q2}, \Delta \mathbf{v}_{q3}, \Delta \mathbf{v}_{q4}\right)^T$$

Δt_{qi} is decision variable i for the moment of the second pulse maneuver $\Delta \mathbf{v}_{qi}, i = 1, 2, 3, 4$ is a four-pulse maneuver vector decision variable.

The path planning model for the intersection of spacecraft and debris is as follows:

$$\min \sum_{q=1}^{N} \sum_{i=1}^{4} \left|\Delta \mathbf{v}_{qi}\right| \tag{5}$$

$$s.t. \quad \mathbf{r}_s^+(t_{qi}) = \mathbf{r}_s^-(t_{qi}), \ q = 1, \ldots, N \ i = 1, \ldots, 4 \tag{6}$$

$$\mathbf{v}_s^+(t_{qi}) = \mathbf{v}_s^-(t_{qi}) + \Delta \mathbf{v}_{qi}, \ q = 1, \ldots, N \ i = 1, \ldots, 4 \tag{7}$$

$$\mathbf{r}_s^+(t_{q4}) = \mathbf{r}_q(t_{q4}), \ q = 1, \ldots, N \tag{8}$$

$$\mathbf{v}_s^+(t_{q4}) = \mathbf{v}_q(t_{q4}), \ q = 1, \ldots, N \tag{9}$$

$$t_{q1} \leq t_{q2} \leq t_{q3} \leq t_{q4} \ q = 1, \ldots, N \tag{10}$$

$$\max_q t_{q4} \leq \mathrm{T}_F, \ q = 1, \ldots, N \tag{11}$$

$$x_{q-1\,q} = 1, \ q = 2, \ldots, N \tag{12}$$

$\mathbf{r}_s^-, \mathbf{v}_s^-, \mathbf{r}_s^+, \mathbf{v}_s^+$, are the position and velocity vector of the spacecraft before and after the orbit change; $\mathbf{r}_q(t), \mathbf{v}_q(t)$ are the position and velocity vector of the No. q fragment at time t. T_F is the latest end of the total task for debris removal. Formula (5) is objective function, that is, the total energy consumption of the debris removal task is the smallest; formula (6) (7) are Pulse thrust model, that is, the spacecraft position vector does not change before and after the pulse is applied, and the velocity vector after the orbit change is the sum of the velocity vector before the orbit change and the pulse vector; formula (8) (9) are end state constraints for rendezvous tasks, In this paper, the single-circle J2 perturbed Lambert algorithm is used to meet the terminal constraints of each rendezvous task; formula (10) represents the time constraint of four-pulse orbit change; formula (11) indicates that the debris removal task needs to be completed within the specified time; formula (12) represents the spacecraft will meet the debris sequentially according to the optimal removal order.

4 Ant Colony Solving Algorithm

The low-orbit space debris removal path planning problem is essentially a mixed integer nonlinear planning problem, which is a NP difficult problem. With the increase of the number of debris to be removed, the traditional precise algorithm cannot find a feasible solution within an acceptable time, so this paper Use intelligent optimization algorithm to solve.

4.1 Classic Ant Colony Optimization Algorithm

Inspired by real ant foraging behavior, Professor M. Dorigo [14] first proposed a bionic evolution algorithm in 1991, called Ant Colony Optimization (ACO). The ACO algorithm is first used to solve the traveling salesman problem (TSP). It uses distributed feedback parallel computing, which is easy to merge with other algorithms and has strong robustness. In 2008, Sochi et al. [17–19] proposed ACO R, which uses the solution in the solution file as a pheromone. The pheromone is updated by the Gaussian kernel function. The algorithm directly extends the ant colony algorithm in the discrete domain to the continuous domain. Because of its global search, positive feedback, group optimization and distributed parallel computing and other characteristics, it has shown outstanding applicability when solving large-scale complex discrete combination optimization problems. Given the excellent performance of ACO in the field of discrete optimization, many scholars Expanding to the field of continuous optimization, with the rapid development of ant colony optimization algorithm, it has received more and more attention, and is used in various fields such as data mining and cloud computing.

This paper will improve a continuous ant colony algorithm, using ACO and continuous domain ACO (ACOR) to solve the upper and lower optimization problems. Due to the rich research results of the ACO algorithm, due to space limitations, this article will not repeat the details of the ACO solution, only the continuous domain ACO solution process is described (Table 1).

4.2 Feasible Solution Construction

At the beginning of each iteration, the ant adopts an incremental solution construction strategy to construct a feasible solution dimension by dimension. When constructing the decision variables of each dimension, the ant uses a two-stage sampling method to sample the Gaussian kernel function corresponding to the decision variables of the dimension. First, according to the weight parameters, a Gaussian sub-function is selected according to the probability; then, by selecting the Gaussian Box-Muller sampling of the sub-function completes the sampling of the Gaussian kernel function corresponding to the decision variable of this dimension.

Let T be the set of k n-dimensional elite solutions, and the second-dimensional decision variables of all elite solutions jointly generate a Gaussian kernel function G^i, where the Gaussian subfunction corresponding to the elite solution s_l is g_l^i; the objective function value of the elite solution s_l is $f(s_l)$, Its relative importance is w_l and the second-dimensional decision variable is s_l^i.

Table 1. ACO_R Solution process pseudocode

Continuous domain ant colony optimization algorithm **ACO_R** ()
Initialization parameters, Pheromones;
while algorithm termination condition not met **do**
for each ant k **do**
Feasible solution construction;
end for
Local search;
Pheromone update;
end while
return Optimal solution s^*

The Gaussian kernel function of the i-to decision variable is defined as follows:

$$G_i(x) = \sum_{l=1}^{k} w_l g_l^i(x) = \sum_{l=1}^{k} w_l \frac{1}{\sigma_l^i \sqrt{2\pi}} e^{-\frac{(x-\mu_1^i)^2}{2(\sigma_1^i)^2}} \tag{13}$$

$$\boldsymbol{\mu}^i = \{\mu_1^i, \ldots, \mu_k^i\} = \{s_1^i, \ldots, s_k^i\} \tag{14}$$

$$\sigma_l^i = \zeta \sum_{e=1}^{k} \frac{\left|s_e^i - s_l^i\right|}{k-1} \tag{15}$$

$$w_l = \frac{1}{qk\sqrt{2\pi}} e^{-\frac{(l-1)^2}{2q^2k^2}} \tag{16}$$

$\zeta > 0$ is the convergence control coefficient. The ζ is smaller, the faster the algorithm will converge. Its function is similar to the pheromone evaporation coefficient in ACO. w_l can be seen as a Gaussian function with an expectation of 1, and a variance qk of. The smaller q is, the more inclined it is to use the optimal elite solution in the solution set to guide the optimization of this iteration, otherwise the tendency is to use any elite solution on average. The parameter q can be used to adjust the global search and local search preferences; l is the ranking of the elite solution s_l in the solution set.

4.3 Pheromone Update

Due to the difference in search space, ACOR cannot inherit ACO's pheromone setting and updating strategy, that is, setting pheromone for each candidate element and updating with a certain strategy. Instead, in the whole optimization process, a certain number of elite solutions are always saved, and the purpose of retaining historical search information is achieved by updating the Gaussian kernel function generated by the elite solutions.

5 Simulation Experiment and Data Analysis

The space debris generated by the disintegration of the Russian Cosmos-3M rocket body is used as an alternative debris removal. Due to the densest space vehicles in this area, and the large mass and volume of these space debris, the potential threat to the space environment is the greatest. Which will get a larger income. According to the cataloging information of the US Strategic Command Space Target Database [20, 21] 2017-1-1 at 00:00:00.000, the space debris of the Russian Cosmos-3M rocket body is distributed by the orbital inclination at 155 space debris at 82 deg (Recorded as 82-deg cluster) and 120 space debris (recorded as 74-deg cluster) with an inclination of 74 deg, the distribution is shown in Fig. 4. In this paper, four LEO debris with an orbital inclination angle of about 82° and the highest priority are selected from the Russian Kosmas 3M rocket disintegration debris library. The number of orbits of the debris to be removed is shown in Table 2. The constant parameters needed in the simulation are expressed as $R_e = 6378.137$ km, $J_2 = 1.0826 \times 10^{-3}$, $\mu_e = 398600.4418$ km^2/s^2. The ant colony algorithm parameter settings are shown in Table 3.

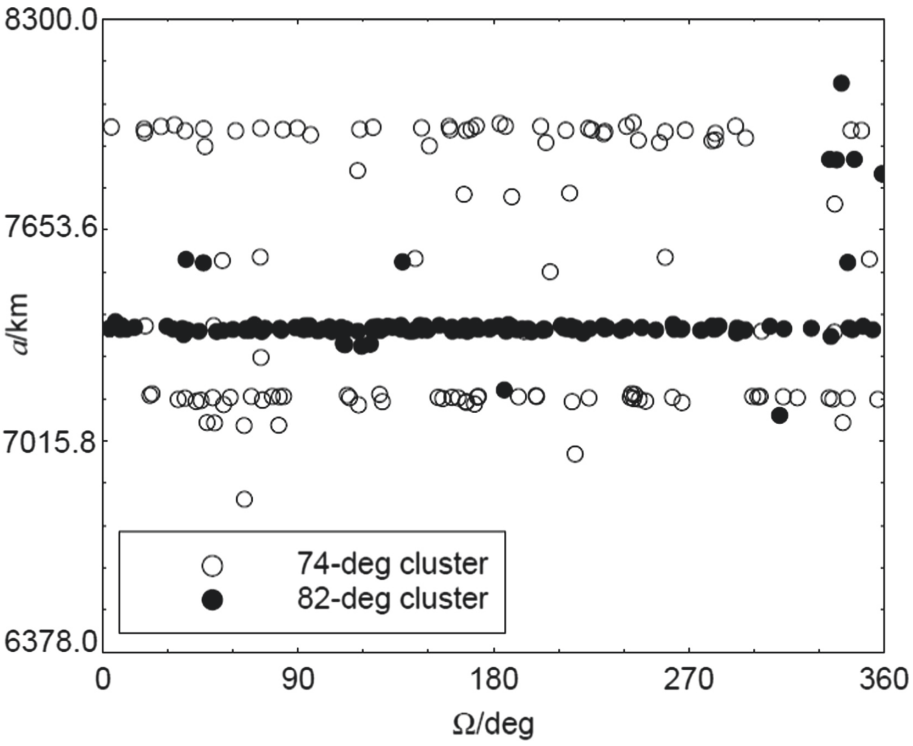

Fig. 4. Cosmos-3MRocket space debris distribution(2017-1-1 00:00:00.000)

Table 2. Track the number of initial orbits of spacecraft and target debris

Target no.	a (km)	e	i (deg)	Ω (deg)	ω (deg)	M (deg)
Clear spacecraft	7376.705	0.004	82.93	183.99	195.09	321.46
Debris 13302	7376.705	0.004	82.93	183.99	195.09	321.46
Debris 5907	7554.527	0.002	82.97	178.76	80.99	138.64
Debris 10138	7364.144	0.002	82.94	189.24	8.79	167.40
Debris 12139	7117.959	0.051	82.95	207.28	113.16	330.25

Table 3. Ant colony algorithm parameters

Parameters	Identifier	ACO	ACO_R
Population size	N	100	20
Maximum evolutionary algebra	MAX_cycle	300	200
Pheromone evaporation coefficient	ρ	0.95	/
Heuristic information, pheromone weight	a, b	3,5	/
Elite solution set size	$N_{archive}$	/	100
Convergence control parameters	ζ	/	0.65
Global search and local search preferences	q	/	10^{-4}

5.1 Upper-Level Planning Results

Based on the spacecraft orbit transfer energy consumption prediction method proposed in Sect. 2.1.1, discrete ACO is used to obtain the optimal debris removal sequence, removal time interval, and orbit transfer energy consumption as shown in Table 4. The optimal debris removal sequence is (13302, 5907, 10138, 12139), the total estimated speed increment is 407.606 m/s, and the total task time is 177.66 d.

Table 4. Debris removal sequence, estimated energy consumption and schedule for each segment

Clear sequence	Estimated transfer energy consumption (m/s)	$t^{op} + t^{wait} + t^{trans}$ (d)
13302 → 5907	88.912	83.516
5907 → 10138	95.101	74.754
10138 → 12139	223.593	28.156

5.2 Lower-Level Planning Results

According to the optimal removal order obtained in the previous section, this section gives the optimal transfer path between the debris of the spacecraft based on the ant colony optimization algorithm section by section. To further test the performance of the algorithm proposed in this paper, Table 5 compares the solution results of ACOR and Differential Evolution (DE) [22]. Figure 5 shows the process of the optimal intersection orbit and orbit height change, where the maneuver time is Refers to the time used by the spacecraft orbital maneuver.

Table 5. Comparison of spacecraft clearance trajectory optimization results

Clear sequence	ACO_R			DE		
	Energy consumption (m/s)	Drift time (d)	Maneuver time (d)	Energy consumption (m/s)	Drift time (d)	Maneuver time (d)
13302 → 5907	**87.22**	83.04	0.77	87.66	83.73	0.04
5907 → 10138	**93.79**	73.55	0.42	100.63	73.05	0.95
10138 → 12139	**187.49**	27.66	0.51	192.86	27.81	0.36

Comparing Tables 4 and 5, it can be seen that no matter the energy consumption is transferred or the interval time is clear, the difference between the exact solution and the estimated value is small, which verifies the effectiveness of the estimated method. It can be seen from Table 5 that the algorithm proposed in this paper is better than the differential evolution algorithm. As can be seen from Fig. 4, the spacecraft intersection fragmentation process is multi-turn transfer, so there are many local optimal solutions, and the optimal results are obtained through calculation examples. Compared with drawing, it shows that ACOR can find the optimal solution that is similar to the estimated solution, which fully verifies the excellent performance of ACOR.

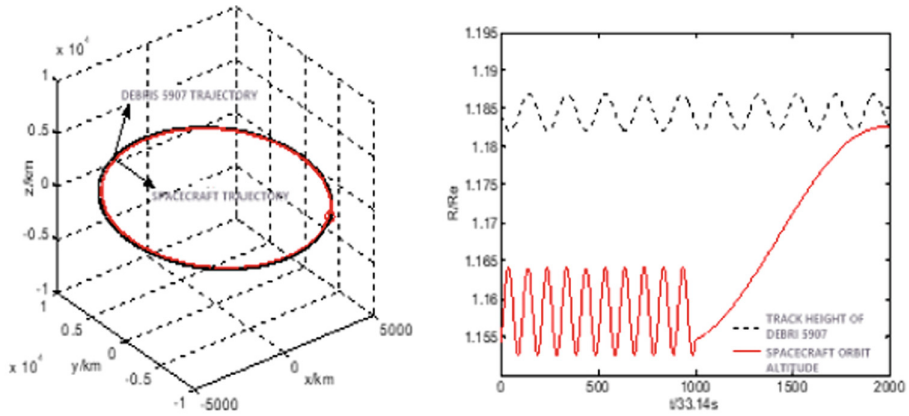

(a) Clearing 5907 debris optimal orbit and orbit height change process

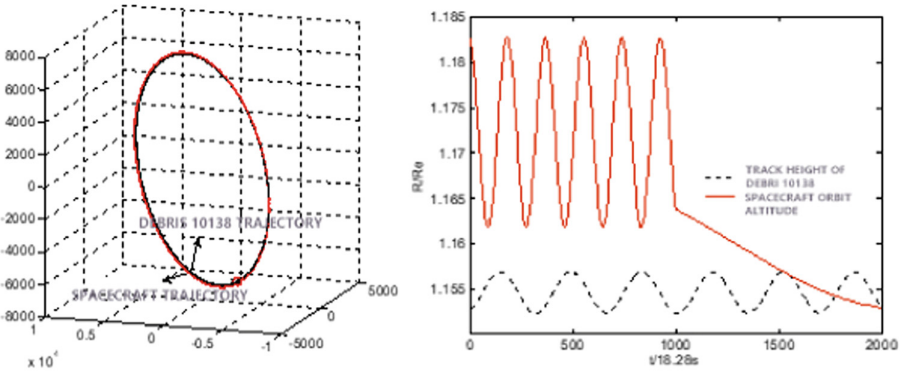

(b) Clearing 10138 debris optimal orbit and orbit height change process

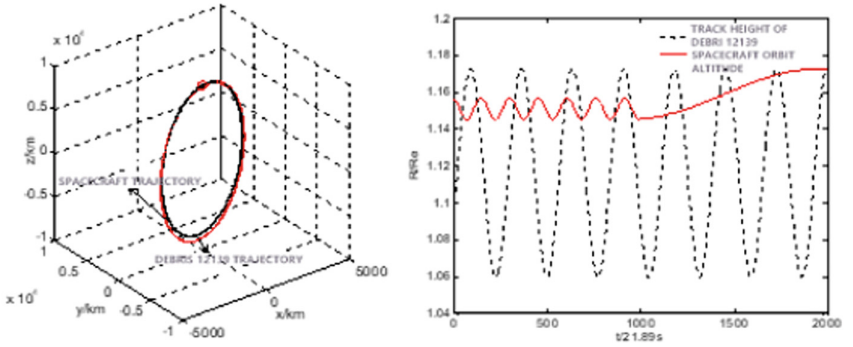

(c) Clearing 12139 debris optimal orbit and orbit height change process

Fig. 5. Optimal orbit and orbit height change process

6 Conclusion

In this paper, a nonlinear programming model for low-orbit multi-space debris removal paths [23] is constructed, and a two-level optimization solution [24] algorithm is designed. A method for estimating spacecraft orbit transfer energy consumption is proposed, and based on this, a fast solution strategy for the optimal order of debris removal and an optimal path planning algorithm for spacecraft removal based on ant colony optimization are proposed. The simulation results verify that the proposed low-orbit multi-debris removal optimal guidance method based on ant colony optimization is feasible and efficient. The research results of this paper provide technical reserves for the follow-up exploration of the integrated design optimization problem of inter-debris transfer orbits and debris detection sequences.

References

1. Lin, X.: Space debris status and cleanup. Spacecr. Eng. **21**(3), 1–10 (2012)
2. Li, Y.: Space Debris Removal. National Defense Industry Press, Beijing (2014)
3. Huo, J.: A survey of space debris. J. Acad. Equip. Command Technol. **18**(5), 56–60 (2007)
4. Weidmann, K.: Space debris mitigation. Chin. Spaceflight **2012**(08)
5. Zhu, W.: Discussion on the application of micro satellite space debris cleaning method. In: 2007 Proceedings of the Conference on System Simulation Technology and Its Application (2007)
6. Liou, J.C.: Collision activities in the future orbital debris environment. Adv. Space Res. **38**(9), 2102–2106 (2006)
7. Johnson, N.L.: Orbital debris: the growing threat to space operations (2010)
8. The NASA Orbital Debris Office. Orbital Debris Quarterly News. Orbital Debris Quarterly News **22**(3) (2018)
9. Kessler, D.J., Johnson, N.L., Liou, J.C., et al.: The Kessler syndrome: implications to future space operations. Adv. Astronaut. Sci. **137**(8), 2010 (2010)
10. Barbee, B.W., Alfano, S., Pinon, E., et al.: Design of spacecraft missions to remove multiple orbital debris objects. In: 2011 Aerospace Conference, pp. 1–14. IEEE (2011)
11. Liou, J.C., Johnson, N.L., Hill, N.M.: Controlling the growth of future LEO debris populations with active debris removal. Acta Astronaut. **66**(5–6), 648–653 (2010)
12. Cerf, M.: Multiple space debris collecting mission—debris selection and trajectory optimization. J. Optim. Theory Appl. **156**, 761–796 (2013)
13. Olympio, J., Frouvelle, N.: Space debris selection and optimal guidance for removal in the SSO with low-thrust propulsion. Acta Astronaut. **93**, 263–275 (2014)
14. Dorigo, M., Maniezzo, V., Colorni, V.: Ant system: optimization by a colony of cooperating agents. IEEE Trans. Syst. Man Cybern.-Part B **26**, 29–41 (1996)
15. Changyan: Correction method of double-impulse intersection orbit for heteroplane elliptical orbit considering J2 camera action. J. Astronaut. **2008**(04)
16. Ge, H.: Pheromone-based adaptive continuous domain hybrid ant colony algorithm. Comput. Eng. Appl. **2017**(06)
17. Socha, K., Dorigo, M.: Ant colony optimization for continuous domains. Eur. J. Oper. Res. **185**, 1155–1173 (2008)
18. Socha, K., Dorigo, M.: Ant colony optimization for continuous domains. Eur. J. Oper. Res. **2006**(3)
19. Socha, K., Dorigo, M.: Ant colony optimization for continuous domains. Eur. J. Oper. Res. **185**(3), 1155–1173 (2008)

20. https://celestrak.com/
21. https://en.wikipedia.org/wiki/North_American_Aerospace_Defense_Command
22. Qin, A.K., Huang, V.L., Suganthan, P.N.: Differential evolution algorithm with strategy adaptation for global numerical optimization. IEEE Trans. Evol. Comput. **13**(2), 398–417 (2009)
23. Lin, M., Xu, M., Fu, X.: A parallel algorithm for the initial screening of space debris collisions prediction using the SGP4/SDP4 models and GPU acceleration. Adv. Space Res. **59**, 2398–2406 (2017)
24. Ferreira, J.C., Fonseca, C.M., Denysiuk, R., Gaspar-Cunha, A.: Methodology to select solutions for multiobjective optimization problems: weighted stress function method. J. Multi-Criteria Decis. Anal. **24**(3–4), 103–120 (2017)